Nematoelasticity of hybrid molecular-colloidal liquid crystals

B. Senyuk,[1] H. Mundoor,[1] I. I. Smalyukh,[1,2,3,4] and H. H. Wensink[5,*]

[1] 030 ,
[2] 030 ,
[3] 030 ,
[4] 030 ,
[5] 502, 1405 ,

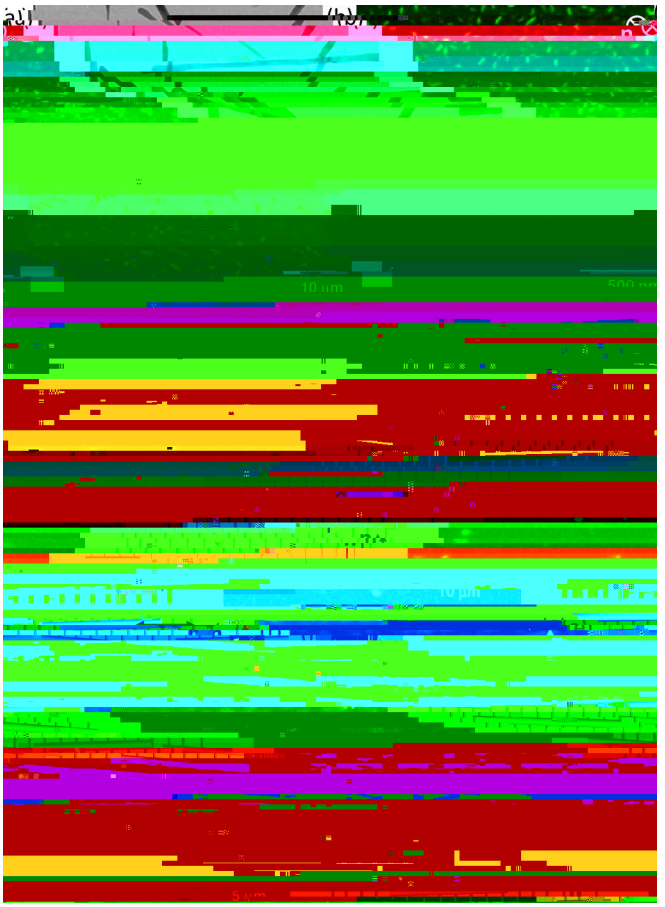

FIG. 1. Structure and composition of a hybrid molecular-rod system: (a) Transmission electron micrograph of colloidal nanorods after acid treatment. (b), (d) Up-conversion-based luminescence confocal microscopy images of the nanorods in a uniaxial nematic LC in a homeotropic (b) and planar (d) cell. (c) Schematic overview and corresponding luminescence confocal microscopy image (d) of the nanorods in a uniaxial nematic LC. (e) Schematic overview and corresponding luminescence confocal microscopy image (f) of the nanorods forming an orthorhombic biaxial nematic LC in a planar cell.

realigning torques with respect to the solvent director, but at the same time weak enough to avoid bulk disclinations or other topological defects around the colloidal surfaces [12]. These defects possess a well-defined topology and are routinely encountered for relatively large nematic colloidal inclusions with strong surface anchoring. They give rise to strong interparticle forces [5] leading to dynamically arrested composites [15,75–78]. In contrast, because of weaker elastic distortions and additional electrostatic stabilization, structure

director field. The latter therefore remains largely intact. The principal impact of the inclusions on the elastic properties of the host LC then stems from the surface-anchoring energy of a single rod, which is enhanced in the presence of weak distortions of the molecular director [89]. Our theoretical predictions are tested against experimental measurements of the splay modulus for low-concentration uniaxial hybrid LCs. We find that our model provides a quantitative prediction of the increase of the splay modulus with the concentration of immersed rods. We note that our study reported here is a first step in exploring the elastic properties of hybrid molecular-colloidal LCs, which in future can be extended to the regimes where particles induce topological defects with significant molecular alignment perturbations around the colloidal particles, both within nematic colloidal dispersions and in cases when smectic, columnar, and crystalline colloidal organizations arise (for the first two, see examples in our recent studies of colloidal disk dispersions in molecular nematic hosts of calamitic mesogens [71]).

The second part of this article (Sec. IV) concerns the elastic moduli of the orthorhombic hybrid LC. We demonstrate that

approaches a simple Gaussian which reads

$$J(\theta) \sim \frac{\sigma}{4\pi} \exp\left(-\frac{\sigma}{2}\theta^2\right) \tag{17}$$

with amplitude

$$\sigma = \frac{\pi}{w_0} \gg 1. \tag{18}$$

As before, knowledge of the rod orientation probability enables us to analyze the two main elastic contributions, the first one mediated by surface anchoring forces and the second one

TABLE I. Classification of the 12 elastic moduli featuring in Eq. (22) of an orthorhombic hybrid rod-molecular system in terms of the principal deformation modes of the individual components and the leading-order contribution from the molecular host (denoted by superscript "0"), surface-anchoring (", "), and rod-correlations (" "). The values given in the last row are based on a hybrid LC with a rod volume fraction of $\varphi \sim 0.1\%$.

elastic modulus:	1	2	3	4	5	6
director-specific deformation:	$\delta\mathbf{n}_1$	$\delta\mathbf{n}_2'''$	$\delta\mathbf{n}_3$	$\delta\mathbf{m}_1$	$\delta\mathbf{m}_2$	$\delta\mathbf{m}_3$
principal modulus:	$K_1^{(0)}$	$K_2^{(0)} + K_2^{(\prime)}$	$K_3^{(0)}$	$K_1^{(\prime)}$	$K_2^{(\prime)}$	$K_3^{(\prime)}$
current experiment:	$K_1^{(0)}$	$K_2^{(0)}$	$K_3^{(0)}$	~ 0	~ 0	$K_3^{(\prime)}$
estimated value (pN):	6.15	3	10	~ 0	~ 0	0.3
elastic modulus:	7	8	9	10	11	12
director-specific deformation:	$\delta\mathbf{m}_3$	$\delta\mathbf{n}_3'''$	$\delta\mathbf{n}_1$	$\delta\mathbf{m}_1$	$\delta\mathbf{n}_2''' + \delta\mathbf{m}_2$	$\delta\mathbf{m}_3 + \delta\mathbf{n}_3$
principal modulus	$K_3^{(\prime)} + K_1^{(0)}$	$K_3^{(0)} + K_1^{(\prime)} + K_3^{(\prime)}$	$K_1^{(0)}$	$K_1^{(\prime)}$	$K_2^{(0)} + K_2^{(\prime)} + K_2^{(\prime)}$	$K_3^{(\prime)} + K_3^{(0)}$
current experiment:	$K_3^{(\prime)} + K_1^{(0)}$	$K_3^{(0)}$	$K_1^{(0)}$	~ 0	$K_2^{(0)}$	$K_3^{(0)} + K_3^{(\prime)}$
estimated value (pN):	6.45	10	6.15	~ 0	3	10.3

A. Classification of the orthorhombic elastic moduli

An intuitive way to rationalize the existence of 12 curvature

limit $\sigma \gg 1$ and $\beta \gg 1$. Up to leading order for small ψ, we find only a nonzero contribution for the splay modulus:

$$\begin{aligned} {}^{(,)}_{1} &\sim \frac{2}{3} w_0 \overline{\varphi}^{2}, \\ {}^{(,)}_{2} &\sim 0, \\ {}^{(,)}_{3} &\sim 0. \end{aligned} \tag{27}$$

The fact that surface anchoring leads to a much stronger enhancement of the splay elasticity than for the uniaxial nematic [cf. Eq. (12)] is not surprising because in the biaxial state the rods are strongly directed along **m** where the impact of a splayed **n** on the homeotropic surface anchoring is the largest (Fig. 3). Although ${}^{(,)}_{1}$ can attain several pN's in magnitude, it does not feature in any of the elastic moduli listed in Table I. The surface anchoring elasticity, therefore, does not affect the nematoelasticity of our orthorhombic hybrid nematic system, at least in the limiting case of strong rod alignment along **m** to which we restrict ourselves here.

C. Elasticity generated by rod correlations

The formation of a stable orthorhombic nematic fluid requires elevated rod concentration where the moduli associated with nanorod correlations ${}^{(\,)}_{}$ ($= 1, 2, 3$) are expected to be much larger than those for the relatively dilute uniaxial nematic. To estimate the extent to which rod interactions dominate the elastic properties of the hybrid LC, we use the scaling predictions shown previously in Eq. (20). We infer that at the highest rod concentration probed in experiment, $\varphi = 0.142\%$, the bend elasticity generated by the charged rods is much smaller than that of 5CB (${}^{(0)}_{3} \approx 10$ pN), so it seems justified to ignore all contributions in Eq. (22) that involve splayed and twisted distortions of **m**.

D. Leading-order moduli for an orthorhombic hybrid nematic

Having demonstrated that both surface-anchoring terms are much weaker than those due to rod-correlations, and noting that the rod-generated splay and twist elastic moduli are negligible compared to the dominant bend modulus, we arrive at the following leading-order estimates:

$$\begin{aligned} {}_{7} &\sim {}^{(0)}_{1} + {}^{(\,)}_{3}, \\ {}_{8} &\sim {}^{(0)}_{3}. \end{aligned} \tag{28}$$

Applying the same approximations to all 12 constants featuring in the continuum theory Eq. (22), we arrive at a much more manageable set of moduli that only depend on the known values for pure 5CB and the bend elastic constant of the immersed rods ${}^{(\,)}_{3}$. We wish to underline that the estimates only make sense for the current hybrid molecular-rod nematic system, which consists of slender rods with particular combination of electrochemical properties regarding surface charge and screening. For instance, the balance between surface anchoring and intercolloidal forces is likely to be quite different for short rods for which surface anchoring contributions play a more prominent role. Also, the bend-splay elastic anisotropy for conventional nematic order is expected to be different in view of the intricate electrostatic interactions between finite-aspect-ratio colloidal particles [103,104]. We reiterate that all predictions presented here are subject to the condition that the rods be strongly aligned along their director **m**.

Going back to the experimental system at hand and recalling that the rod-driven bend modulus ${}^{(\,)}_{3} \approx 0.28$ pN is still an order of magnitude smaller than the smallest elastic modulus

combination of several moduli) of the orthorhombic material that we will explore below.

We start from the magnetization **M** of a single uniaxial rod (of either molecular or colloidal origin) with orientation **n** characterized by a parallel diamagnetic susceptibility ($\chi_\parallel$) and a perpendicular one ($\chi_\perp$) with respect to the principal rod axis in response to an applied magnetic field **H** [107]:

$$\mathbf{M} = \mu_0[\chi_\parallel(\mathbf{n}\otimes\mathbf{n}\cdot\mathbf{H}) + \chi_\perp(\mathbf{I}-\mathbf{n}\otimes\mathbf{n})\cdot\mathbf{H}$$

$$\text{VI}: \quad {}^{*} = \sqrt{\frac{2}{\varphi_0 \chi^{(0)}}},$$

$$\text{VI}_{\text{w}}: \quad {}^{*} = \sqrt{\frac{6 + 7}{\varphi \chi^{( )}}},$$

$$\text{VI}_{\text{r}}: \quad {}^{*} = \begin{cases} \sqrt{\frac{1 + 9 + 11}{\varphi_0 \chi^{(0)}}}, \\ \sqrt{\frac{5 + 6 + 12}{\varphi \chi^{( )}}}, \end{cases} \tag{A12}$$

and

$$\text{VII}: \quad {}^{*} = \sqrt{\frac{1}{\varphi_0 \chi^{(0)}}},$$

$$\text{VII}_{\text{w}}: \quad {}^{*} = \begin{cases} \sqrt{\frac{2 + 11}{\varphi_0 \chi^{(0)}}}, \\ \sqrt{\frac{11}{\varphi \chi^{( )}}}, \end{cases}$$

$$\text{VII}_{\text{r}}: \quad {}^{*} = \sqrt{\frac{4}{\varphi \chi^{( )}}}. \tag{A13}$$

Wherever two expressions are given, only the one giving the lowest threshold magnetic field * will be of physical significance. From the setups described thus far, we are able to identify the following six moduli:

$$\begin{aligned} \text{III} &\rightarrow {}_1, \\ \text{IV}_{\text{w}} &\rightarrow {}_2, \\ \text{II} &\rightarrow {}_4, \\ \text{IV}_{\text{r}} &\rightarrow {}_5, \\ \text{III}_{\text{r}} &\rightarrow {}_{11}, \\ \text{IV or VI}_{\text{r}} &\rightarrow {}_9. \end{aligned} \tag{A14}$$

Furthermore, if one could design a setup in which the Fréedericksz transition of **m** precedes that of **n**, one could extract $_{10}$ via

$$\text{V}_{\text{r}} \text{ or IV} \rightarrow {}_{10}. \tag{A15}$$

The last five modes can be obtained as follows. First, upon close inspection of Eq. (22) one deduces that $_7$ and $_8$ represent a bend deformation of **m** specifically along the direction **n** and a bend deformation of **n** along **m**, respectively. The corresponding bend moduli for the systems $_6$ and $_3$

[25] V. M. Pergamenshchik and V. A. Uzunova, Phys. Rev. E **83**, 021701 (2011).
[26] C. P. Lapointe, T. G. Mason, and I. I. Smalyukh, Science **326**, 1083 (2009).

[90] J. P. Straley, Phys. Rev. A **8**, 2181 (1973).
[91] T. Odijk, Liq. Cryst. **1**, 553 (1986).
[92] B. Senyuk, Q. Liu, S. He, R. D. Kamien, R. B. Kusner, T. C. Lubensky, and I. I. Smalyukh, Nature (London) **493**, 200 (2013).
[93] M. Kléman and O. D. Lavrentovich, (Springer, Berlin, 2003).
[94] P. G. de Gennes and J. Prost, (Clarendon Press, Oxford, 1993).
[95] R. G. Priest, Phys. Rev. A **7**, 720 (1973).
[96] M. P. Allen, G. T. Evans, D. Frenkel, and B. M. Mulder, Adv. Chem. Phys. **86**, 1 (1993).
[97] J. V. Selinger, Liq. Cryst. Rev. **6**, 129 (2018).
[98] A. Rapini and M. Papoular, J. Phys. Colloq. **30**, C4-54 (1969).
[99] T. Odijk, Macromolecules **19**, 2313 (1986).